

Observing random walks of atoms in buffer gas through resonant light absorption

Kenichiro Aoki* and Takahisa Mitsui†

Research and Education Center for Natural Sciences and Department of Physics, Hiyoshi, Keio University, Yokohama 223–8521, Japan

(Received 24 May 2016; published 18 July 2016)

Using resonant light absorption, random-walk motions of rubidium atoms in nitrogen buffer gas are observed directly. The transmitted light intensity through atomic vapor is measured, and its spectrum is obtained, down to orders of magnitude below the shot-noise level to detect fluctuations caused by atomic motions. To understand the measured spectra, the spectrum for atoms performing random walks in a Gaussian light beam is computed, and its analytical form is obtained. The spectrum has $1/f^2$ (f is frequency) behavior at higher frequencies, crossing over to a different, but well-defined, behavior at lower frequencies. The properties of this theoretical spectrum agree excellently with the measured spectrum. This understanding also enables us to obtain the diffusion constant, the photon cross section of atoms in buffer gas, and the atomic number density from a single spectral measurement. We further discuss other possible applications of our experimental method and analysis.

DOI: [10.1103/PhysRevA.94.012703](https://doi.org/10.1103/PhysRevA.94.012703)

I. INTRODUCTION

Thermal motion is inevitable for any object at finite temperatures. On the microscopic scale, perhaps the most well known example is the Brownian motion of particles, which is optically visible [1–3]. Even on a smaller scale, the thermal motions of the atoms are visible through surface fluctuations of liquids [4–6], high-power interferometry measurements on mirrors [7], and complex materials [8]. In gases, the ballistic thermal motion of atoms and molecules leads to the transit time broadening of the resonant widths [9], and the free streaming of atoms can be observed through their transit noise in light [10]. When atoms have relatively shorter mean free paths, such as when buffer gas is present, we expect the atoms to perform random-walk behavior caused by collisions with other atoms and molecules. This has been seen only indirectly through spin-relaxation methods [12–15] and from the resulting diffusion [16]. Our main objective is to observe the random-walk behavior of the atoms themselves directly.

Perhaps the most direct way to see objects is just to shine light on the object and observe its absorption or scattering. This is precisely what is performed in this experiment. We measure light absorption of atoms transiting a beam of light. There are, however, a number of theoretical and technical obstacles that need to be overcome. First, any observation affects the observed, and it is difficult to directly observe each collision and the free motion of an atom between collisions without qualitatively changing their motion since the particles performing the measurement have momenta $\sim h/\lambda$, where λ is the mean free path or smaller. While this is a fundamental quantum-mechanical principle, we can still use photons with smaller momenta, which have longer wavelengths, to directly observe atoms undergoing random-walk behavior, through their absorption spectra. The fluctuations in these spectra clearly reflect the motions of the atoms. Such a direct measurement has not been performed previously to our knowledge, and this is what we accomplish in this work.

Experimentally, light was shone on rubidium atoms in nitrogen buffer gas. The light frequency was tuned to a resonance of the rubidium atoms; the transmitted power of light was measured, and its fluctuations were analyzed [Fig. 1(a)]. While this is, in principle, simple, the fluctuations need to be measured down to orders of magnitude below the shot-noise level, or the standard quantum limit, to uncover the spectra. Shot noise is the quantum statistical noise in the number of detected photons of the light beam transmitted through the cell, which contributes to the photocurrent power spectrum as $2eI$ (e is the electron charge, I is the photocurrent). To obtain the spectrum to the desired precision, the experiment is configured so that statistical analysis involving correlation analysis is applicable. To understand the observed behavior, we compute the spectrum of atoms performing random walks in a light beam theoretically and derive its form analytically. The theoretical spectra are compared to the experimentally observed spectra, and their properties are found to be in excellent agreement.

We describe the concept and the setup of the experiment briefly in Sec. II, explain the theory behind the power spectrum of atoms performing random walks in a Gaussian light beam in Sec. III, and analyze the experimentally measured spectra in view of the theory in Sec. IV. We end with conclusions and discussions in Sec. V.

II. DESIGN AND SETUP OF THE EXPERIMENT

The basic concept underlying our experiment, shown in Fig. 1(a), is to just measure the fluctuations in the light transmitted through atoms and molecules in a cell. In our experiment, the cells contain rubidium atoms and nitrogen molecules which serve as the buffer gas. The obtained fluctuation spectrum is

$$S(f) = \frac{1}{T_{\text{meas}}} |\tilde{\mathcal{P}}(f)|^2, \quad \tilde{\mathcal{P}}(f) = \int_0^{T_{\text{meas}}} dt e^{-i2\pi f t} \mathcal{P}(t), \quad (1)$$

where \mathcal{P} is the power of the transmitted light and the tilde denotes its Fourier transform [17]. f is the frequency, and T_{meas} is the measurement time. In practice, however, the setup

*ken@phys-h.keio.ac.jp

†mitsui@phys-h.keio.ac.jp

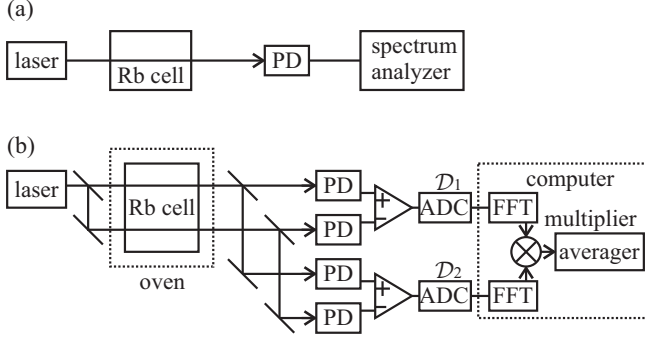


FIG. 1. Configuration of the experiment: a resonant laser light beam is shone through a rubidium cell, its transmitted power is measured by the photodetectors (PD), and the power fluctuation spectrum is computed. (a) The conceptual design of the experiment. (b) The setup used in the measurements. Differential measurement from the two beams is used to remove the correlated noise (+−), and the correlations of the transmitted power from the same beam $\mathcal{D}_1, \mathcal{D}_2$ are used to extract the signal (see text). The photodetector outputs are converted to a digital signal by the analog to digital converters (ADC), Fourier transforms are performed (FFT), and then correlations are computed and averaged. FFT and averagings are performed on a computer.

in Fig. 1(a) by itself is not sufficient to extract the spectrum. This spectrum will be almost completely buried under other unwanted noise, in particular the shot noise. Often referred to as the “standard quantum limit,” shot noise is usually a limiting factor in the precision of photometric measurements [18]. Therefore, to achieve the desired results, sophisticated noise-reduction methods need to be performed to remove the shot noise, along with laser noise and the other extraneous noise, to levels which allows us to recover the fluctuation spectrum. This full experimental design is shown in Fig. 1(b). Resonant light is shone through a cell (depth $d_z = 44$ mm, diameter of 44 mm) containing rubidium atoms in nitrogen buffer gas. The rubidium atoms are at saturation density, and the nitrogen gas has a pressure of 200 Torr. To reduce the unwanted noise, we compute the correlations of the measurements from two independent photodetector measurements $\mathcal{D}_1, \mathcal{D}_2$ of the same atomic vapor. The shot noises in $\mathcal{D}_{1,2}$ are independent, so that

$$\langle \overline{\mathcal{D}_1 \mathcal{D}_2} \rangle \longrightarrow |\tilde{S}|^2 \quad (\mathcal{N} \rightarrow \infty), \quad (2)$$

where $\langle \dots \rangle$ denotes averaging and the relative statistical error here is $1/\sqrt{\mathcal{N}}$, with \mathcal{N} being the number of averagings [8]. This statistical reduction can reduce any *uncorrelated* noise, including shot noise, to any desired level, in principle. There is another technical complication in that unwanted *correlated* noise, such as laser noise, also appears. This was removed through differential measurement, using the measurements from two light beams, as seen in Fig. 1(b). The light beams were separated by 15 mm in this experiment. The averagings of correlations of Fourier-transformed transmitted power measurements, combined with the differential measurements, allowed us to extract the desired spectra, Eq. (1). The incoming light was tuned to the ^{85}Rb - D_2 transition from the hyperfine levels $5^2S_{1/2}$ to $5^3P_{3/2}$ [19] and was circularly polarized using a quarter-wave plate. The beam radius w was measured

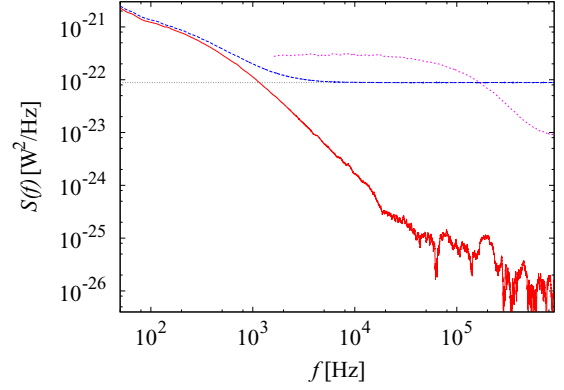


FIG. 2. An observed spectrum with and without correlation measurements (solid red and dashed blue lines, respectively). Without the correlation measurement, the spectrum reduces to the shot-noise level at higher frequencies. Shot-noise level is also shown (grey dots). Some extraneous noise still remains at higher frequencies. $\mathcal{P} = 58 \mu\text{W}$, $w = 0.34$ mm, and temperature was 46.4°C in this measurement. For comparison, the transit-noise spectrum of the rubidium gas without buffer gas with the same w and similar \mathcal{P} is also shown for $f > 1.6$ kHz ($\mathcal{P} = 68 \mu\text{W}$, short-dashed magenta line).

with a linear image sensor (Hamamatsu Photonics S9227), and transmitted power was measured using photodiodes (PD, Hamamatsu Photonics S5973), as in Fig. 1. Light beams with powers \mathcal{P} of 0.1–1 mW and radius $w = 0.3$ –1 mm were used, and the typical measurement times were around 2000 s. A similar experimental setup was used to measure the transit noise, Rabi noise, and Zeeman noise of rubidium atoms without the buffer gas [10], and its principle of noise reduction is explained in more detail in [11].

In our experiment, S is generated by atoms transverse the beam and will be referred to as the transit noise below. The transit-noise spectra are calibrated using the shot-noise spectra measured by the photodetector. An example of the obtained spectrum is shown in Fig. 2, in which the transit noise was acquired down to four orders of magnitude below the shot-noise level. This spectrum qualitatively differs from that of atoms freely streaming across the beam, which is also shown.

III. SPECTRUM OF ATOMS PERFORMING RANDOM WALKS

Let us now compute the spectrum of atoms performing random walks in a Gaussian beam of light. The form of the fluctuation spectrum is determined by the movement of the individual atoms in a light beam with inhomogeneous intensity. The electric field strength $\mathcal{E}(x, y)$ and the intensity of a monochromatic Gaussian light beam $I(x, y)$ with the angular frequency $\omega = 2\pi f$ are

$$\begin{aligned} \mathcal{E}(x, y) &= \mathcal{E}_0 e^{ikz - i\omega t}, & I(x, y) &= I_0 e^{-2(x^2 + y^2)/w^2}, \\ I_0 &= \frac{1}{2} c \epsilon_0 \mathcal{E}_0^2, \end{aligned} \quad (3)$$

where the light-beam direction was taken to be along the z axis, w is the beam radius, and $ck = \omega$. ϵ_0 and c are the permittivity and the speed of light in vacuum. When resonant light is shone

on it, an atom radiates as a dipole with the power,

$$\wp(t) = \frac{\mu_{Rb}^2 \omega}{4\hbar} |\mathcal{E}(x, y)|^2 \frac{\Gamma}{(\Delta\omega + kv_z)^2 + \Gamma^2/4}. \quad (4)$$

Here, x, y is the location of the atom in the x, y plane, v_z is the velocity of the atom in the beam direction, μ_{Rb} is the dipole moment of the atom, $\Delta\omega$ is the amount of detuning, and Γ is the linewidth. In our experiments, the light is tuned to the resonance, and due to the effect of the buffer gas, the linewidth is larger than the Doppler shift effect kv_z , so that the dipole radiation power can be well described by

$$\wp(t) \simeq \sigma I(x, y), \quad \sigma = \frac{2\mu_{Rb}^2 \omega}{\hbar c \epsilon_0 \Gamma}. \quad (5)$$

The expression for σ is the standard formula for the photon absorption cross section [20], except for the natural width being replaced by Γ . In this picture, we are treating the electromagnetic fields semiclassically, which ignores saturation effects. Under the conditions of our experiments, the lifetime of atoms in the excited states is short due to collisions with buffer-gas molecules, making this treatment appropriate.

Since atoms radiate the absorbed light in all directions independently, they reduce the forward light transmission. The power spectrum, Eq. (1), for the fluctuations in the transmission of a Gaussian light beam that has passed through atomic vapor can be obtained by summing over the power radiated by the atoms, Eq. (5), as

$$\begin{aligned} S(f) &= \frac{1}{T_{\text{meas}}} \left| \sum_j \int_0^{T_{\text{meas}}} dt e^{-i\omega t} \sigma I(x_j(t), y_j(t)) \right|^2 \\ &= \frac{1}{T_{\text{meas}}} (\sigma I_0)^2 \sum_j \int_0^{T_{\text{meas}}} dt \int_0^{T_{\text{meas}}} dt' e^{-i\omega(t-t')} \\ &\quad \times e^{-2[x_j(t)^2 + y_j(t)^2]/w^2} e^{-2[x_j(t')^2 + y_j(t')^2]/w^2}. \end{aligned} \quad (6)$$

Here, the sum is over the atoms, which are labeled by j . The atoms are performing the random walks in the buffer gas independently, so their motions are uncorrelated. This property was used here. From here on, we drop the cumbersome index j . An atom performing a random walk travels as

$$x(t) = x_0 + \Delta x(t), \quad \Delta x(t) \equiv \int_{t_0}^t dt' \xi(t'), \quad x_0 = x(t_0). \quad (7)$$

Here, $\xi(t)$ satisfies

$$\langle \xi(t) \xi(t') \rangle = 2D \delta(t - t'), \quad (8)$$

where D is the diffusion constant and $\langle \dots \rangle$ denotes statistical averaging. Similar relations exist also for y . The sum of the contributions of atoms can be computed by first averaging over the random walks, $\Delta x = \Delta x(t), \Delta x' = \Delta x(t')$, using their probability distribution $P(\Delta x, \Delta x')$. Since random walks in each dimension are independent, we may treat spatial dimensions x, y separately in the averaging. For the x direction,

$$\begin{aligned} \langle e^{-2(x^2(t) + x^2(t'))/w^2} \rangle &= \int d\Delta x d\Delta x' P(\Delta x, \Delta x') \\ &\quad \times e^{-2[(x_0 + \Delta x)^2 + (x_0 + \Delta x')^2]/w^2}. \end{aligned} \quad (9)$$

The distribution is Gaussian in these two variables, with the probability distribution

$$\begin{aligned} P(\Delta x, \Delta x') &= \frac{1}{2\pi |R|^{1/2}} \exp \left[-\frac{1}{2|R|} (R_{22} \Delta x^2 + R_{11} \Delta x'^2 \right. \\ &\quad \left. - 2R_{12} \Delta x \Delta x') \right], \end{aligned} \quad (10)$$

where $|R| = R_{11}R_{22} - R_{12}^2$. Using the properties of random walks, Eq. (8), we derive

$$\begin{aligned} \langle (\Delta x)^2 \rangle &= 2D|t - t_0| = R_{11}, \quad \langle (\Delta x')^2 \rangle = 2D|t' - t_0| = R_{22}, \\ \langle \Delta x \Delta x' \rangle &= 2D \min(|t - t_0|, |t' - t_0|) = R_{12}. \end{aligned} \quad (11)$$

The integration, Eq. (9), is Gaussian, and a straightforward but cumbersome calculation yields

$$\begin{aligned} \langle e^{-2[x^2(t) + x^2(t')]/w^2} \rangle &= \left(1 + 4 \frac{(R_{11} + R_{22})}{w^2} + 16 \frac{|R|}{w^4} \right)^{-1/2} \\ &\quad \times \exp \left(-4 \frac{x_0^2}{w^4} \frac{w^2 + 2(R_{11} + R_{22}) - 4R_{12}}{1 + 4(R_{11} + R_{22})/w^2 + 16|R|/w^4} \right). \end{aligned} \quad (12)$$

By combining the x and y directions and replacing the sum over the atoms in the spectrum, Eq. (6), by $nd_z \int dx_0 \int dy_0$, where n is the number density of atoms, we arrive at the following final compact form for the spectrum:

$$\begin{aligned} S(f) &= \frac{\pi}{4} nd_z \sigma^2 I_0^2 w^2 \int_{-\infty}^{\infty} d\tau \frac{e^{-i\omega\tau}}{1 + 4D|\tau|/w^2} \\ &= \frac{\pi nd_z \sigma^2 I_0^2 w^4}{8D} \text{Re}[-e^{i\omega'} \text{Ei}(-i\omega')]. \end{aligned} \quad (13)$$

Here, we let $t \rightarrow -\infty$, $\text{Ei}(x)$ is the exponential integral function [21], and $\omega' = \omega w^2/(4D)$. The $1/T_{\text{meas}}$ factor cancels one of the integrals in the formula for the spectrum, Eq. (6), since the integrand depends only on the time difference $t' - t$. Formula (13) is the transmission power spectrum of atoms individually performing random walks in a Gaussian light beam. Since

$$\text{Re}[-e^{i\omega'} \text{Ei}(-i\omega')] = \frac{1}{\omega'^2} - \frac{6}{\omega'^4} + O\left(\frac{1}{\omega'^6}\right), \quad (14)$$

we obtain the high-frequency behavior of the spectrum as

$$S(f) = \frac{C(w, n, \mathcal{P})}{f^2} + \dots, \quad C(w, n, \mathcal{P}) = \frac{2n\sigma^2 d_z \mathcal{P}^2 D}{\pi^3 w^4}. \quad (15)$$

The theoretical spectrum, Eq. (13), is uniquely determined from the properties of atoms and the experimental parameters. It should be noted that the diffusion constant D appears in the spectrum, directly reflecting the motion of atoms. The shape of the spectrum is governed by D and w , while the overall coefficient further depends on \mathcal{P}, n . While the spectrum was derived with atoms in mind, it should be evident that the spectrum is applicable to any light-absorbing particles performing random walks in a Gaussian beam.

IV. OBSERVED SPECTRA OF ATOMS IN BUFFER GAS

We shall now compare the properties of the spectrum derived in the previous section with the spectra observed experimentally, as explained in Sec. II. We first analyze the properties of the system in our experimental situation, partly to understand concretely the background for the approximations made in the previous section. Rubidium atoms are in nitrogen buffer gas at 200 Torr at temperatures of 40 °C to 50 °C. The average velocity of a rubidium atom is 300 m/s, the Doppler width is 320 MHz, and the width of the rubidium atoms in nitrogen buffer gas is $\Gamma/(2\pi) = 3.7$ GHz [22], which is about 600 times larger than the natural width [19]. In the buffer gas, the width of the rubidium resonance is larger than the hyperfine level splittings, thereby reducing the system to a two-level system to a good approximation. Due to collisional broadening, $kv_z/(2\Gamma) \sim 0.04$, so Doppler effects are small in Eq. (4), as mentioned above. The ratio of photon momentum to the average rubidium atom momentum is about 3×10^{-5} , making the measurement essentially passive. Light beams with powers $\mathcal{P} \lesssim 2$ mW and beam radii w of 0.2 to 1 mm were used. The diffusion constant for the rubidium atoms in nitrogen buffer gas at 200 Torr is $D = 1.59(4) \times 10^{-5}$ m²/s [15]. Then, the transit time for an atom across a light beam with $w = 1$ mm is around 4 ms. The average number of photons absorbed by an atom during this transit is $\mathcal{P}\sigma/(2h\nu D)$, which is interestingly independent of the beam size. This number is around 2×10^3 for $\mathcal{P} = 1$ mW under our experimental conditions. Due to the short excited-state lifetime, the ratio of atoms in the excited state is $(\mu_{Rb}\mathcal{E}/\hbar\Gamma)^2 \sim 2 \times 10^{-5}$ for $\mathcal{P} = 1$ mW, $w = 1$ mm, so saturation effects should be negligible in our measurements.

There are several distinct properties of the theoretical spectrum, Eq. (13):

- (1) The shape of the spectrum is independent of \mathcal{P} .
- (2) $S(f) \sim 1/f^2$ for $f \gg D/w^2$ but has different behavior at lower frequencies, so D can be extracted from the spectrum.
- (3) $S(f)$ is proportional to \mathcal{P}^2 and w^{-4} .
- (4) $S(f)$ is proportional to $n\sigma^2$, from which $n\sigma^2$ can be measured.

We shall now investigate these properties in the experimental results: While some physical properties of atoms were provided above as a background, we shall use only the quantities measured in our experiments, \mathcal{P} , w , d_z , and the experimental spectra in this analysis, unless noted otherwise. The transit-noise spectra for the buffered rubidium gas is shown in Fig. 3 for powers \mathcal{P} varying more than over an order of magnitude. One overall coefficient, $C(w, n, \mathcal{P})$, has been extracted from each experimental spectrum by fitting to $1/f^2$ at higher frequencies. From the shape of the measured spectra, $D = 6.0 \times 10^{-5}$ m²/s was obtained. The theoretical spectra are compared to the experimentally measured ones in Fig. 3, and they are all seen to agree quite well. D obtained here is quite consistent with the previously measured values [15]. The measured spectra divided by the overall coefficient $C(w, n, \mathcal{P})$ are shown in Fig. 3 (inset). Theoretically, the rescaled spectra should be identical, which they are to a high degree.

The dependence of $C(w, n, \mathcal{P})$ on \mathcal{P} is shown in Fig. 4. The \mathcal{P}^2 behavior is shown and clearly fits the experimental results quite well. This behavior, which shows no saturation effects, is consistent with the short lifetime of the excited state, as mentioned above. The spectrum, Eq. (13), is proportional

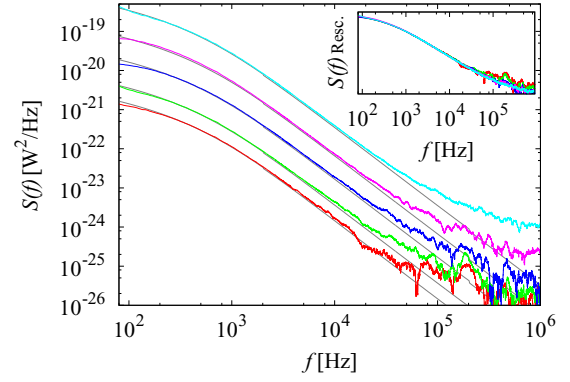


FIG. 3. Power spectra of rubidium atoms in nitrogen gas (200 Torr) and the corresponding theoretical spectra (thin gray lines), Eq. (13). The spectra have larger magnitudes for larger light power \mathcal{P} . The theoretical and experimental spectra agree well. Inset: the experimental spectra rescaled by their overall coefficient, which show that the shapes of the spectra are the same to a high degree. The vertical scale is denoted as “ $S(f)$ Resc.,” and the units on the vertical scale are arbitrary. $\mathcal{P} = 58.0$ (red), 92.8 (green), 197 (blue), 429 (magenta), and 912 (cyan) μ W. $w = 0.96$ mm, and the temperature of the gas is 46.4 °C. Larger \mathcal{P} leads to a larger signal.

to n/w^4 , so that if values of $C(w, n, \mathcal{P})$ are rescaled by the inverse values of n/w^4 , they should all agree. It can be seen that this is indeed the case in Fig. 4 (inset). For this rescaling, the number densities n_{theory} from the literature [19] were used. These properties agree with those of the theoretical spectrum, Eq. (13), and show that the coefficient $C(w, n, \mathcal{P})$ is a function of \mathcal{E}_0 for a Gaussian beam. It should be recalled, however, that the shape of the spectrum is rather governed by w and D .

Since the spectrum, Eq. (13), is uniquely determined from the properties of the atoms and the experimental conditions, both n and σ can be extracted from the results as follows. By applying Beer’s law [20] for the transmission rate $\exp(-n\sigma d_z)$, we can extract $n\sigma$ for each experiment using the measured transmission rate. Then, $n\sigma^2$ can be obtained from $C(w, n, \mathcal{P})$

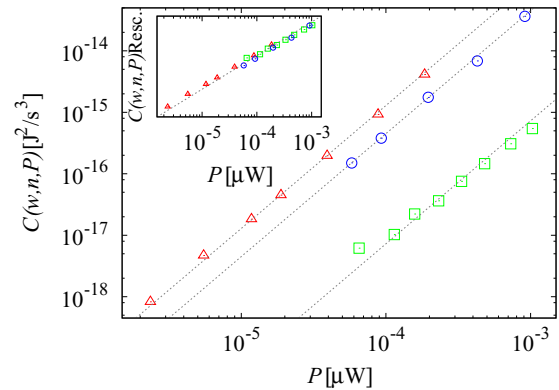


FIG. 4. Power \mathcal{P} dependence of $C(w, n, \mathcal{P})$: $C(w, n, \mathcal{P})$ and fits to them proportional to \mathcal{P}^2 (gray dashed lines) are plotted for measurements at the following temperatures and w values: 44.6 °C, 0.96 mm (\square), 46.4 °C, 0.34 mm (\circ), and 50.0 °C, 0.34 mm (\triangle). Inset: \mathcal{P} dependence of $C(w, n, \mathcal{P})w^4/n_{\text{theory}}$ for the same spectra and its fit to \mathcal{P}^2 (gray dashed line). The data can be seen to fall on a single line. The vertical scale is labeled as “ $C(w, n, \mathcal{P})$ Resc.,” and arbitrary units are used.

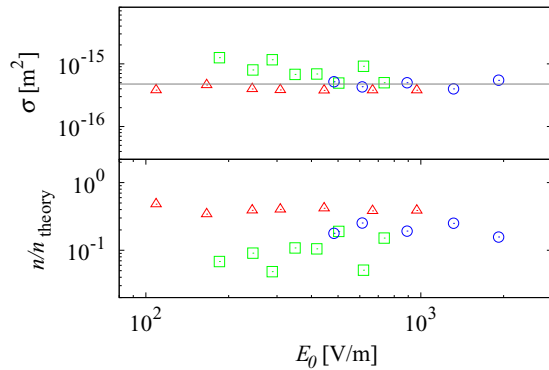


FIG. 5. Cross section σ and the rubidium number density n extracted from the spectra used in Fig. 4 (the same symbols are used). Top: measured σ . The theoretical cross section, Eq. (5), is shown (gray solid line). Bottom: measured rubidium number density n relative to the number density in the literature n_{theory} .

from experimentally measured physical parameters. Combining these data, we arrive at σ, n values extracted from each set of spectrum and transmission rate measurements, which we show in Fig. 5. The measured cross section is compared to the theoretical formula in Eq. (5), using the linewidths in [22], and the density n is compared to the theoretical rubidium vapor saturation density [19]. \mathcal{P} , w , and the temperature were measured independently of the spectra, and the theoretical and experimental results agree reasonably. Compared to the relative properties analyzed above, the absolute values of the spectra are much more sensitive to various uncertainties, both experimental and theoretical.

Here, n and σ are both seen to be independent of \mathcal{E}_0 within experimental uncertainties, as would be expected for nonsaturated vapor. The photon absorption cross section of atoms in buffer gas has not been directly measured to our knowledge, and the simple formula (5) seems to be a good approximation. While the system should be effectively a two-level system due to collisional broadening, more detailed analysis may be necessary to establish the numerical factors precisely. Some of the more significant experimental uncertainties also should be mentioned: The power of the light beam entering the cell and transmitted light can differ by up to 60%, and the intensity of the beam changes along the beam itself. In this work, we have consistently used the transmitted power of light measured by the photodetectors [Fig. 1(b)] when referring to the power of the light beam \mathcal{P} . Furthermore, the incoming and the transmitted light beams are not perfectly Gaussian, and the temperature of the gas inside the cell, which affects the number density of atoms, can have uncertainties of a few degrees throughout the whole measurement.

V. DISCUSSION

In this work, the time-dependent fluctuations of the light transmission power of atoms in buffer gas were experimentally measured, down to four orders of magnitude below the shot-noise level in their spectra. On the theoretical side, the spectrum of atoms performing random walks in buffer gas was investigated, and an analytic form of the spectrum was derived. The theoretical spectrum was found to describe the observed spectra quite well.

From a measured spectrum and the transmission rate, the diffusion constant D , the number density of the rubidium atoms n , and the photon absorption cross section of the atom in buffer gas σ can all be obtained. Namely, we can obtain D from the shape of the spectrum, $n\sigma$ from the absorption rate, and then $n\sigma^2$ from the overall size of the spectrum. In typical experimental situations, the combination $n\sigma$ can be measured from absorption but not n and σ separately. This is a distinct feature of the fluctuation measurement, and we believe that it is interesting and practical to be able to measure these quantities at the same time, so that the same experimental conditions are guaranteed.

In the theory of the spectrum of atoms performing random walks, we used a semiclassical picture. This seems to us to be the simplest approach and one that should be applied first. It also seems to describe the observed spectra remarkably well. Since the Doppler width is much smaller than the linewidth and the monochromatic light is tuned to the resonance, the assumption that atoms are in resonance is reasonable. It was tacitly assumed that σ^2 in the spectrum, Eq. (13), is the square of σ found in the average transmission rate. However, the time scale for deexcitation is 3×10^{-10} s, and the decay time is probabilistic for individual atoms. The cross sections used in the absorption rate and in the spectrum, Eq. (13), should therefore be regarded as averaged values. Furthermore, this time scale is a factor of 15 smaller than the time scale obtained from the diffusion constant in [15], $6D/v^2 \sim 4 \times 10^{-9}$ s (v^2 is the average velocity squared of rubidium atoms in three spatial dimensions). While the deexcitation time scale needs not be identical to the diffusion time scale, they both come from atoms colliding with buffer-gas molecules. It is possible that there are corrections, perhaps including quantum electrodynamics contributions, to the semiclassical picture presented above which would be of considerable interest. We believe that the transit-noise measurements could provide a way to address these questions in more detail. We also find it fascinating that we can make direct observations of atoms performing random walks.

Since the method we use to measure the transit noise of atoms has not been used previously, it allows us to investigate the validity of the standard basic physics principles, which we feel is important and was also done here. Furthermore, a new method of measurement can open up new approaches to understanding atom-photon interactions. We expect this conceptually simple method to bring about further insight into their properties. Our approach of measuring transit noise is applicable to any atoms or molecules, regardless of the density, pure or mixed, as long as a resonant light source is used. In particular, the properties of atoms in buffer gas and rubidium atoms have played an important role in various active areas of fundamental fields of study in physics, such as atomic clocks [23,24] and Bose-Einstein condensation of cold atoms [25], as well as some applications in other fields [26]. Methods to analyze the properties of atom-photon interactions are of interest also from such considerations.

ACKNOWLEDGMENTS

K.A. was supported in part by the Grant-in-Aid for Scientific Research (Grant No. 15K05217) from the Japan Society for the Promotion of Science (JSPS), and a grant from Keio University.

- [1] R. Brown, *Philos. Mag.* **4**, 161 (1828).
- [2] A. Einstein, *Investigations on the Theory of the Brownian Movement* (Dover, New York, 1956).
- [3] M. Smoluchowski, *Ann. Phys. (Berlin, Ger.)* **326**, 756 (1906).
- [4] M. von Schmoluchowski, *Ann. Phys. (Berlin, Ger.)* **25**, 225 (1908); L. Mandelstam, *ibid.* **41**, 609 (1913).
- [5] D. Langevin, *Light Scattering by Liquid Surfaces and Complementary Techniques* (Marcel Dekker, New York, 1992).
- [6] H. J. Lauter, H. Godfrin, V. L. P. Frank, and P. Leiderer, *Phys. Rev. Lett.* **68**, 2484 (1992); A. Vailati and M. Giglio, *Nature (London)* **390**, 262 (1997).
- [7] K. Numata, M. Ando, K. Yamamoto, S. Otsuka, and K. Tsubono, *Phys. Rev. Lett.* **91**, 260602 (2003); E. D. Black *et al.*, *Phys. Lett. A* **328**, 1 (2004).
- [8] T. Mitsui and K. Aoki, *Phys. Rev. E* **80**, 020602(R) (2009).
- [9] W. Demtröder, *Laser Spectroscopy* (Springer, Berlin, 2008).
- [10] T. Mitsui and K. Aoki, *Eur. Phys. J. D* **67**, 213 (2013).
- [11] T. Mitsui and K. Aoki, *J. Opt. Soc. Am. B* **31**, 195 (2014).
- [12] W. Franzen, *Phys. Rev.* **115**, 850 (1959).
- [13] X. Zeng, Z. Wu, T. Call, E. Miron, D. Schreiber, and W. Happer, *Phys. Rev. A* **31**, 260 (1985).
- [14] M. E. Wagshul and T. E. Chupp, *Phys. Rev. A* **49**, 3854 (1994).
- [15] K. Ishikawa and T. Yabuzaki, *Phys. Rev. A* **62**, 065401 (2000).
- [16] M. Parniak and W. Wasilewski, *Appl. Phys. B* **116**, 415 (2014).
- [17] C. W. Gardiner, *Handbook of Stochastic Methods* (Springer, Berlin, 1985).
- [18] P. Meystre and M. Sargent, III, *Elements of Quantum Optics* (Springer, Berlin, 1990).
- [19] D. A. Steck, <http://steck.us/alkalidata>.
- [20] C. J. Foot, *Atomic Physics* (Oxford University Press, New York, 2005).
- [21] I. S. Gradshteyn and I. M. Ryzhik, *Table of Integrals, Series, and Products* (Academic, New York, 1994).
- [22] M. D. Rotondaro and G. O. Perram, *J. Quant. Spectrosc. Radiat. Transfer* **57**, 497 (1997).
- [23] L. Essen and J. V. L. Parry, *Nature (London)* **176**, 280 (1955); N. Huntemann, M. Okhapkin, B. Lipphardt, S. Weyers, Chr. Tamm, and E. Peik, *Phys. Rev. Lett.* **108**, 090801 (2012); C. J. Campbell, A. G. Radnaev, A. Kuzmich, V. A. Dzuba, V. V. Flambaum, and A. Derevianko, *ibid.* **108**, 120802 (2012).
- [24] A. D. Ludlow, M. M. Boyd, J. Ye, E. Peik, and P. O. Schmidt, *Rev. Mod. Phys.* **87**, 637 (2015).
- [25] M. H. Anderson, J. R. Ensher, M. R. Matthews, C. E. Wieman, and E. A. Cornell, *Science* **269**, 198 (1995); C. C. Bradley, C. A. Sackett, J. J. Tollett, and R. G. Hulet, *Phys. Rev. Lett.* **75**, 1687 (1995); K. B. Davis, M. O. Mewes, M. R. Andrews, N. J. van Druten, D. S. Durfee, D. M. Kurn, and W. Ketterle, *ibid.* **75**, 3969 (1995).
- [26] M. S. Albert, G. D. Cates, B. Driehuys, W. Happer, B. Saam, C. S. Springer, Jr., and A. Wishnia, *Nature (London)* **370**, 199 (1994).